Available online at www.sciencedirect.com
ScienceDirect
Journal of the European Ceramic Society 27 (2007) 1259–1265
www.elsevier.com/locate/jeurceramsoc

Analysis of micro-machining characteristics of Si_3N_4-hBN composites

M.W. Cho [a,*], D.W. Kim [a], W.S. Cho [b]

[a] *Division of Mechanical Engineering, Inha University, Incheon 402-751, Republic of Korea*
[b] *Division of Material Science, Inha University, Incheon 402-751, Republic of Korea*

Available online 7 November 2006

Abstract

In this study, micro-machining characteristics of Si_3N_4-hBN composites were analyzed for the development of micro-pattern making methods. First, Si_3N_4-hBN composite specimens of various h-BN contents were prepared using hot-press method. *R*-Curve behavior of the composites was investigated to understand its machinability. And, micro-shaping, micro-end-milling and micro-drilling processes were performed for the machinability evaluation of the composites. In the micro-shaping, V-grooves were machined and their shapes and cutting forces were measured and analyzed. Similar processes were preformed for the micro-end-milling and micro-drilling processes. The results of this study can be applied to determine optimum micro-machining conditions for Si_3N_4-hBN composites.

Keywords: Machinable ceramics; Si_3N_4-hBN composites; Micro-machining; Micro-shaping; Micro-end-milling; Micro-drilling

1. Introduction

Si_3N_4 composites are known as very difficult-to-cut materials because of its high strength and hardness. Their machining mechanism is much different with metals, which can be characterized by cracking and brittle fracture due to relatively high strength and temperature resistance.[1,2] However, Si_3N_4-hBN composite materials are well known as one of the machinable ceramics, which can be easily machined with hard-alloy cutting tools under proper machining conditions.[3–5] Also, the needs for micro-parts using such materials are rapidly increasing in related application fields.

In this study, the analysis of micro-machining characteristics of Si_3N_4-hBN composites were performed to determine optimum micro-machining conditions for those applications. As a first step, the *R*-curve behavior of the Si_3N_4-hBN composites was investigated to understand its machinability. It could be observed that the *R*-curve rose slowly for this material so that the fracture toughness was low at small cracks but high at long cracks. Then, a set of micro-machining experiments, such as micro-grooving, micro-end-milling and micro-drilling, were performed to investigate the micro-machining characteristics with variable h-BN contents and different conditions. Also, cutting forces and tool wear were investigated for each experimental condition. From the results, it could be investigated that the cutting forces decreased and tool life increased with the increase of h-BN contents. It can be concluded that the results of this study can be applied for the micro-parts production using Si_3N_4-hBN composites.

2. Composites

2.1. Composite processing and microstructure

The starting powders were Si_3N_4 (α-crystal phase > 95%, average particle size, 0.17 μm, Ube Industries, Ltd., Japan), and h-BN (>99% pure, 10 μm, Kojundo Chemical Laboratory Ltd., Japan). The amounts of added h-BN ranged from 0 to 30 vol.%. In all specimens, 8 mol% of Y_2O_3 (>99.9% pure, <0.5 μm, Shinestu Chemical Co. Ltd., Japan) and 6 mol% Al_2O_3 (>99.99% pure, 0.39 μm, Sumitomo Chemical Co. Ltd., Japan), were added as sintering aids. The powders were mixed by wet ball-milling using Al_2O_3 jar, Si_3N_4 balls and ethanol for 72 h. The mixed wet powders were dried on a hot plate using a rotating stirrer to avoid gravity-induced segregation. To obtain fully dense compacts, the dried and sieved (to 16 mesh) powders were hot-pressed at 1800 °C for 2 h under a pressure of 25 MPa in a N_2 atmosphere. Rectangular specimens (3 mm × 4 mm × 36 mm) were prepared by cutting, grinding, and polishing the hot-pressed compact. According to the results of XRD analysis for monolithic Si_3N_4 and Si_3N_4-hBN composites, the phase transi-

* Corresponding author. Tel.: +82 32 860 7306; fax: +82 32 868 1716.
E-mail address: chomwnet@inha.ac.kr (M.W. Cho).

0955-2219/$ – see front matter © 2006 Published by Elsevier Ltd.
doi:10.1016/j.jeurceramsoc.2006.08.002

tion of α- to β-Si_3N_4 was completed in all specimens, and there was no evidence for the reaction between hBN and Si_3N_4 matrix.

The fracture surfaces and polished/etched surfaces of specimens were investigated by SEM. Si_3N_4 grain size was measured from the SEM images of surfaces etched for 1 h by mixed solution of $HF + HNO_3$ at 80 °C. Based on the results for grain size observation, the microstructures of monolithic Si_3N_4 and Si_3N_4-hBN composite revealed a needle-like fine

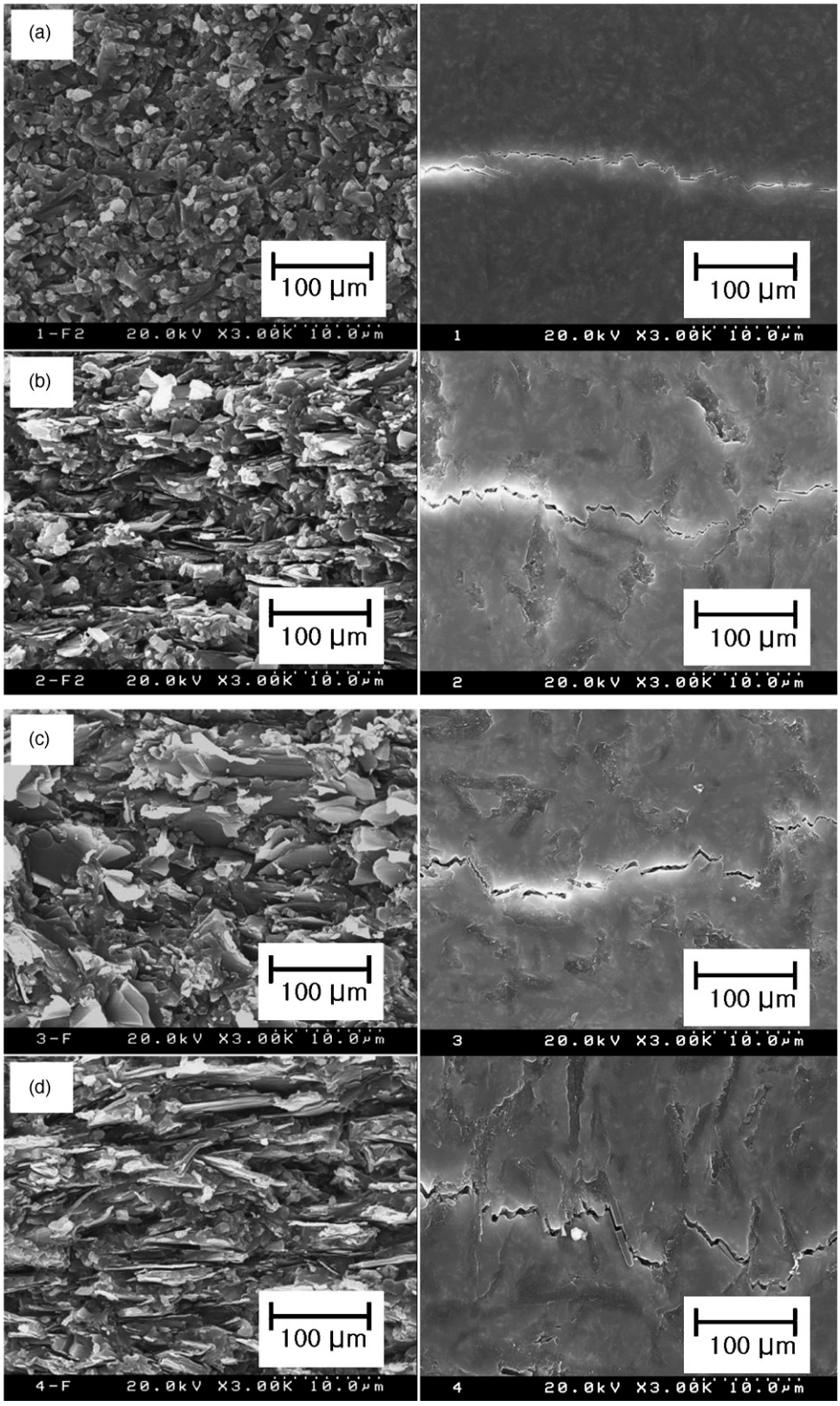

Fig. 1. SEM micrographs of fracture surfaces and crack paths by indentation of (a) 0 vol.%, (b) 20 vol.%, (c) 25 vol.% and (d) 30 vol.% of h-BN.

β-Si_3N_4 grains. The true length of the fine β-Si_3N_4 grains was difficult to measure because the Si_3N_4 grains were oriented three-dimensionally. Thus, the apparent length was measured from the two-dimensional microstructure. The length of β-Si_3N_4 slightly decreased with increasing h-BN content from about 3.2 μm of monolith to 2.8 μm of Si_3N_4-30% BN composite.

Fig. 1 shows the fracture surfaces, broken parallel to the hot-pressed direction, of the monolithic Si_3N_4 and the Si_3N_4-hBN composites. In all specimens, evidence for pullouts of Si_3N_4 grains and h-BN platelets was observed. Also, the crack paths, obtained by indentation, are shown in Fig. 1 for the same specimens. The well-polished surface was indented along the vertical direction to the hot-pressed direction. Crack paths were obtained on the polished section by indentation with a Vickers hardness tester under a load of 196 N. The crack paths in all specimens were sinusoidal due to grain pullout and bridging of grains during crack propagation. Grain bridging enhances fracture toughness resulting in crack resistance behavior (*R*-curve behavior) as fracture toughness increases with crack growth. It is notable that crack paths for Si_3N_4-hBN composites were sinusoidal in larger scales compared with the crack path for Si_3N_4 monolith. Grain bridging at a larger scale leads to more effective toughening.[6]

Based on these microstructural observations, grain bridging and pullout could be possible toughening mechanisms for the monolithic Si_3N_4 as well as Si_3N_4-hBN composite. In general, hot-pressed Si_3N_4-hBN composites exhibit strong texture of BN grains oriented with the *c*-axis parallel to hot-pressing direction. This anisotropic texture may enhance fracture toughness further of the composites by more effective crack bridging and pull-out of grains oriented vertically to the crack propagating direction.

2.2. *R*-Curve behavior analysis for machinability evaluation

For the *R*-curve characterization, indentation under loads from 4.9 to 196 N was employed on the polished surfaces, and 4-point flexural strength was determined. *R*-Curves were obtained from the relationships of the indentation load, indentation crack length and the strength after indentation following the Krause's procedure.[7] Fig. 2 presents the indentation strength as a function of indentation load, and *R*-curves were obtained from the data. For the monolithic Si_3N_4, fracture toughness rises rapidly at the relatively short cracks and saturates to a plateau quickly. On the other hand, the Si_3N_4-hBN composites show slowly rising *R*-curves. At small crack lengths cracks should form and grow easily along the layer-structured BN particles resulting in very low fracture toughness. As cracks grow, grain bridging becomes effective to enhance fracture toughness. The addition of BN particles resulted in the larger scale of grain bridging as shown in Fig. 1, and the plateau fracture toughness was even higher than the monolithic Si_3N_4. This slowly rising *R*-curve behavior could be very important for the machinability of these composites. BN particles in the composites decrease significantly the fracture toughness of the composite at small crack

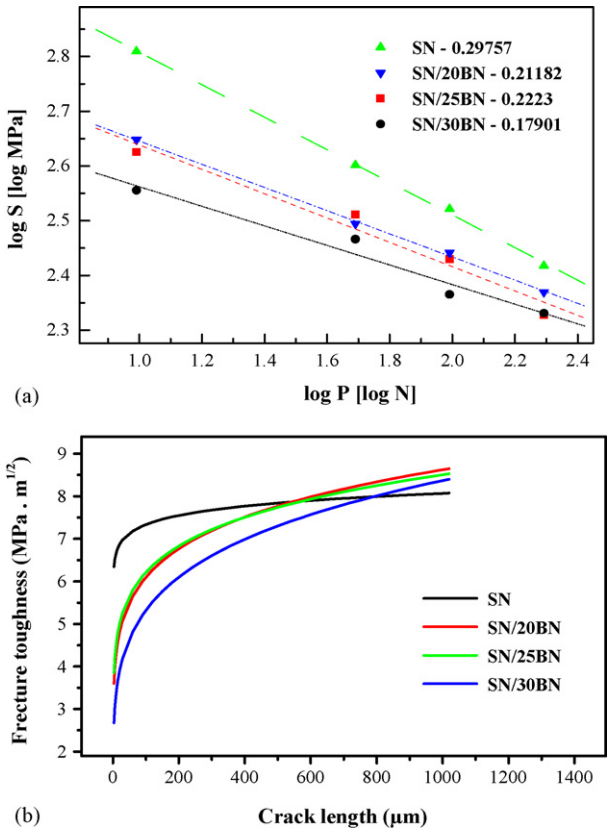

Fig. 2. (a) Indentation load vs. strength and (b) *R*-curves for monolithic Si_3N_4 and Si_3N_4-hBN composites containing 20 vol.%, 25 vol.% and 30 vol.% of h-BN.

lengths, which renders machinability. On the other hand, high fracture toughness at large crack lengths owing to the large-scale grain bridging minimize catastrophic failure or machining damage.

3. Experiments and results

3.1. System setup for micro-machining processes

A micro-machining stage used for this study is illustrated in Fig. 3. The stage has three-directional moving slides; *X*- and *Y*-axis with 200 mm × 200 mm strokes and 5 nm resolution, *Z*-axis with 100 mm stroke and 40 nm resolution. Also, it has two rotating spindles; an air-bearing spindle for milling and drilling processes with maximum 70,000 rpm, a crossing spindle for turning process with 0–6000 rpm range. A tool dynamometer is implemented on the *XY* table to measure cutting forces during the micro-machining processes. Measured cutting force signals are sent to data acquisition system through charge amplifier to analyze the micro-machining process characteristics. Fig. 4 illustrates possible micro-machining processes using the micro-machining stage.[8–11]

3.2. Machinability evaluation in micro-shaping process

First, micro-shaping experiments were performed to form micro-V-grooves using the shaping tools with 90° inclination

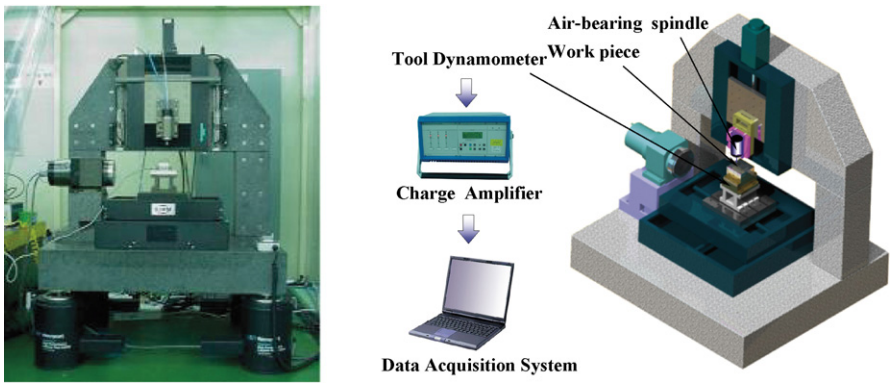

Fig. 3. Micro-machining stage for the experiments.

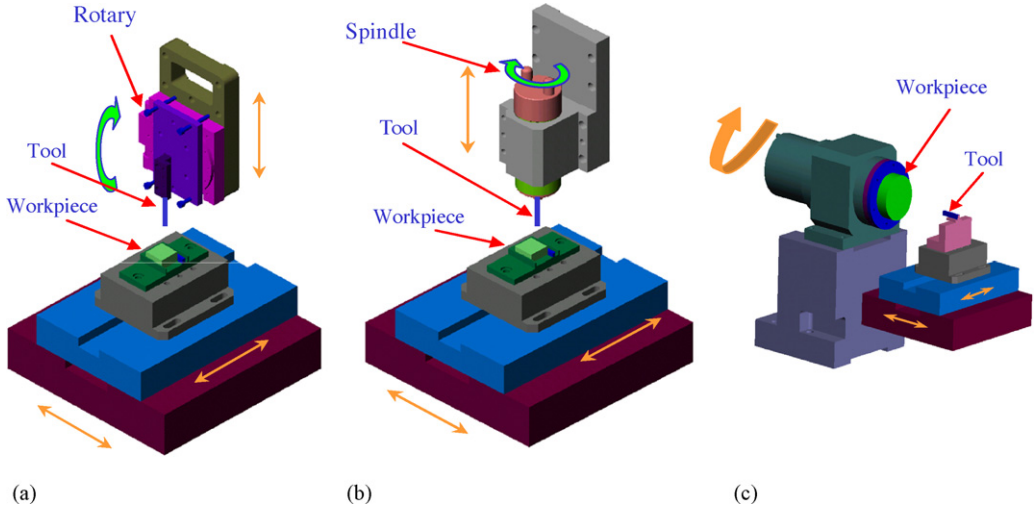

Fig. 4. Possible machining processes using the micro-stage: (a) shaping, (b) milling, drilling and (c) turning.

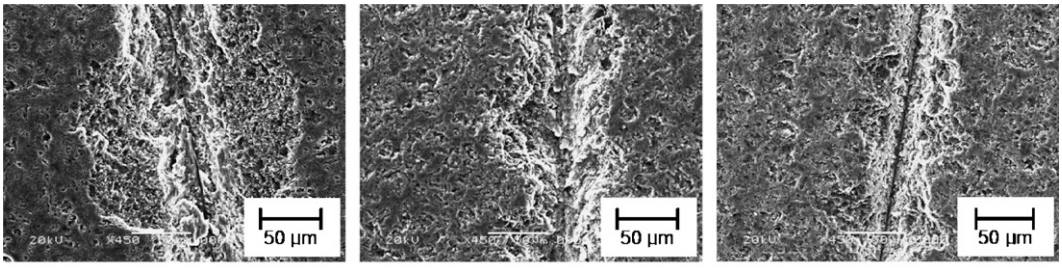

Fig. 5. SEM photographs of machined grooves: (a) 10 vol.% BN, (b) 20 vol.% BN and (c) 30 vol.% BN.

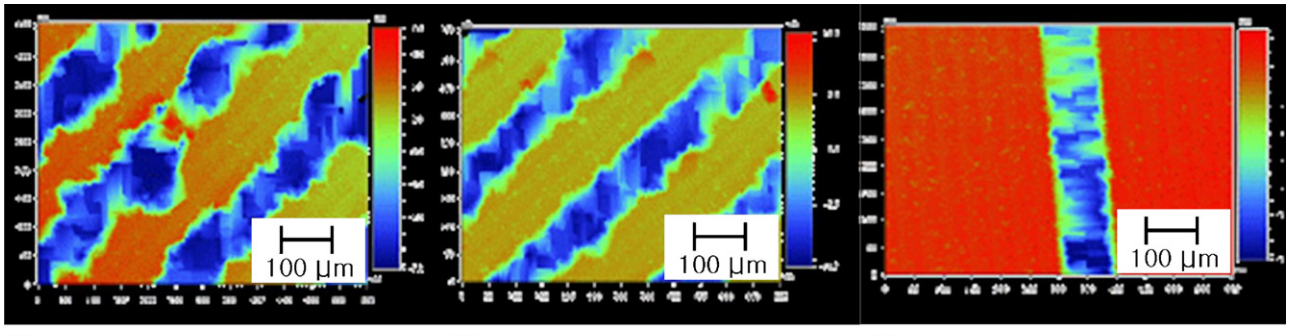

Fig. 6. Measured 3D groove shapes using surface profiler: (a) 10 vol.% BN, (b) 20 vol.% BN and (c) 30 vol.% BN.

Table 1
Micro-V-groove shaping conditions

	Feed: 25	Feed: 50	Feed: 100	Feed: 25 (step)
h-BN (10 vol.%) h-BN (20 vol.%) h-BN (30 vol.%)	Depth: 30 μm	Depth: 30 μm	Depth: 30 μm	Depth: 10 μm for each step

Feed = mm/min.

angle. Imposed shaping conditions for prepared composite specimen are shown in Table 1. Fig. 5 shows the SEM photographs of machined V-grooves using micro-shaping methods for various BN contents when federate = 5 mm/min. Fig. 6 shows measured 3D shapes of grooves using non-contact type surface profiler. From the figures, it could be observed that sharper and cleaner groove edges could be obtained as the h-BN contents in the composites increased. Such phenomenon was due to much more brittle fractures occur during shaping processes as the h-BN contents decrease. Fig. 7 shows measured cutting force variations according to h-BN contents. It could be seen that cutting forces decreased as the h-BN contents increased. Such results correspond to the *R*-curve behavior analysis results as shown in Fig. 2.

3.3. Machinability evaluation in micro-end-milling process

As a next experiment, machinability of the composite was evaluated for micro-end-milling process. Micro-end-milling

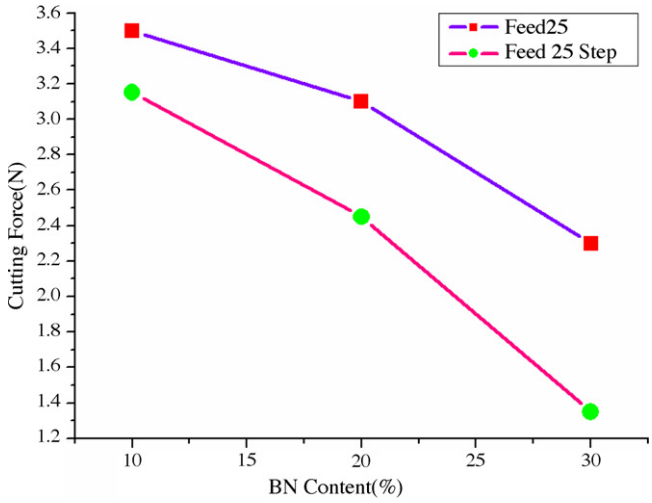

Fig. 7. Cutting forces variations according to BN contents.

method was applied to form micro-barriers with flat-type end mills. Machined barrier widths are 80 and 1000 μm. Fig. 8 shows the SEM photographs of the machined micro-barriers. It could be observed that generally clear barriers were formed. However, when h-BN contents were low, brittle fractures resulted in collapse or crack of the barrier boundaries as shown in Fig. 9(a). It was observed that serious tool wear occurred when machining low vol.% of h-BN composite (5%) as shown in Fig. 10.

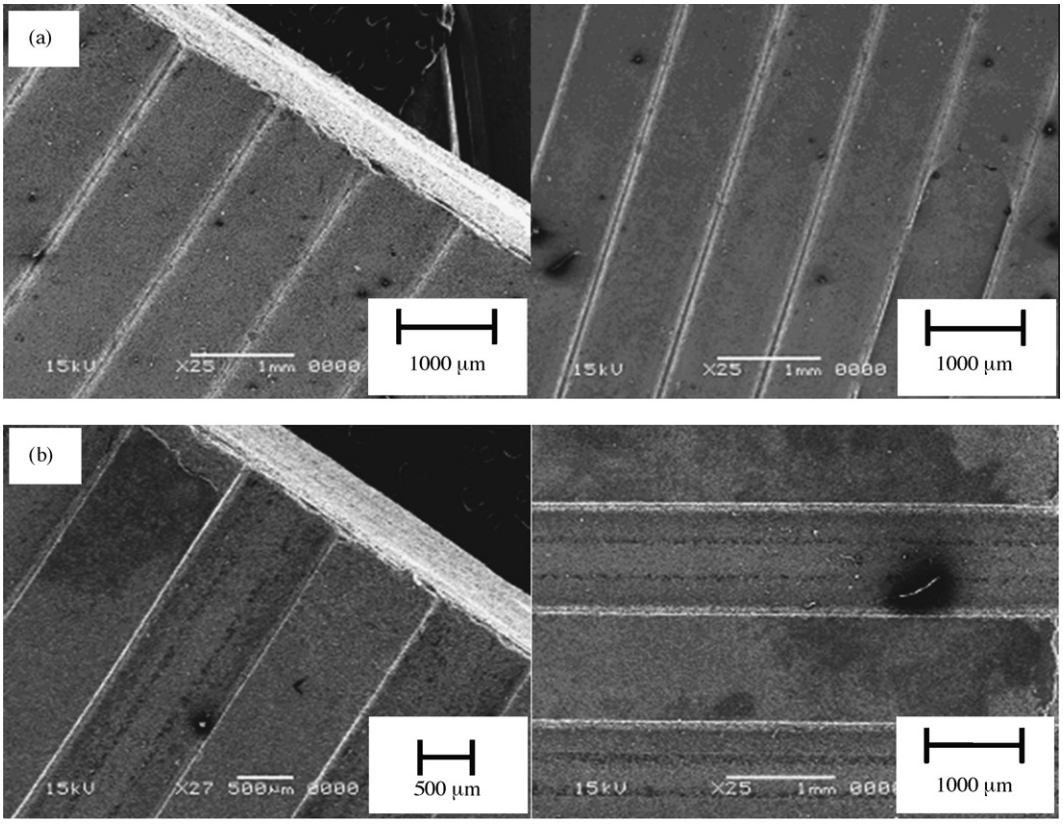

Fig. 8. Micro-barriers machined using micro-end-milling method: (a) barrier width: 80 μm and (b) barrier width: 1000 μm.

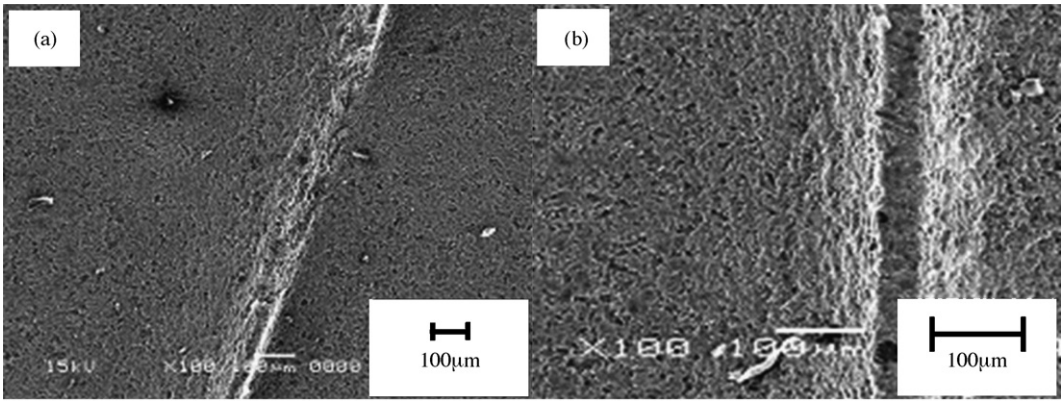

Fig. 9. SEM photographs of machined surfaces (barrier width: 80 μm): (a) 10 vol.% BN and (b) 20 vol.% BN.

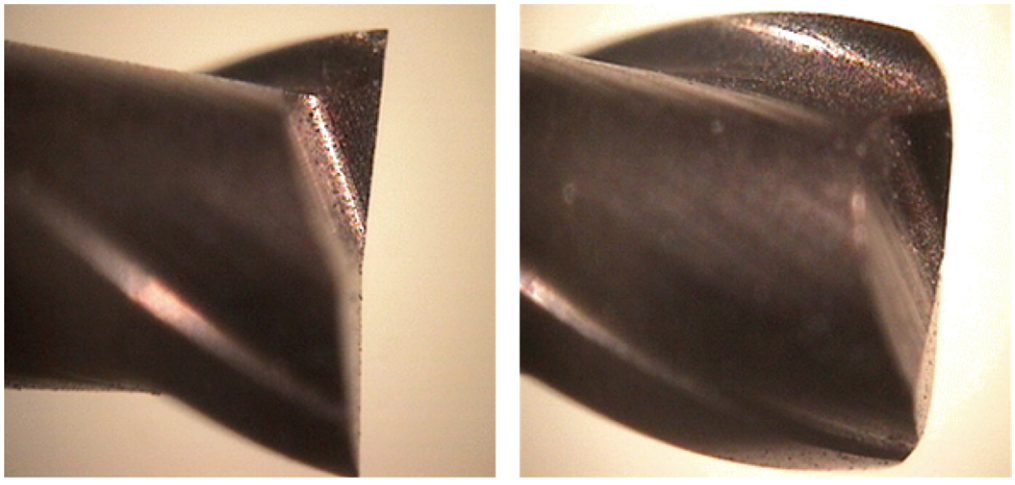

Fig. 10. Tool wear by micro-machining of machinable ceramics (5 vol.% of h-BN): (a) before and (b) after.

3.4. Machinability evaluation in micro-drilling process

Finally, machinability of the composite was evaluated in micro-drilling process. For the experimental works, a micro-drilling system was used, which consists of a high-speed air spindle (max. 60,000 rpm). The drilling process was divided into a certain number of steps and a drill was fed into the composite repetitively until reach the desired depth. Such method allows to avoid micro-drill fracture problems and to easily discharge chips and heats. Drills of 100 μm diameter were used for the experiment, and thrust forces were measured using tool dynamometer under several conditions. The measured results are shown in Fig. 11. Fig. 12 shows the cutting force variations for different conditions. From the figure, it could be observed that the thrust force decreases as spindle rpm increases.

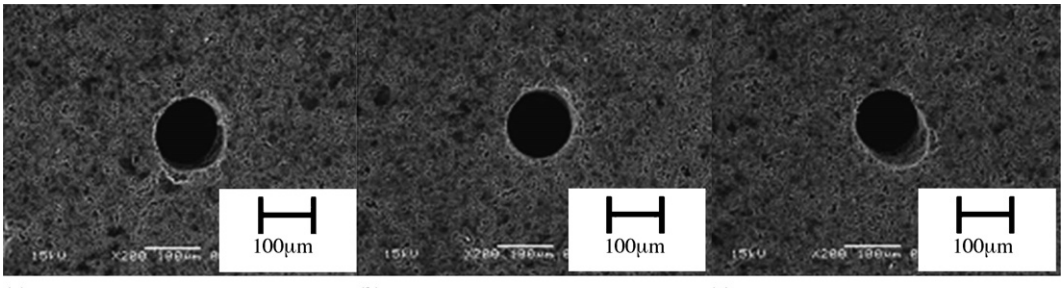

Fig. 11. Drilled micro-holes using 100 μm drill for 30 vol.% BN: (a) 40,000 rpm, (b) 50,000 rpm and (c) 60,000 rpm.

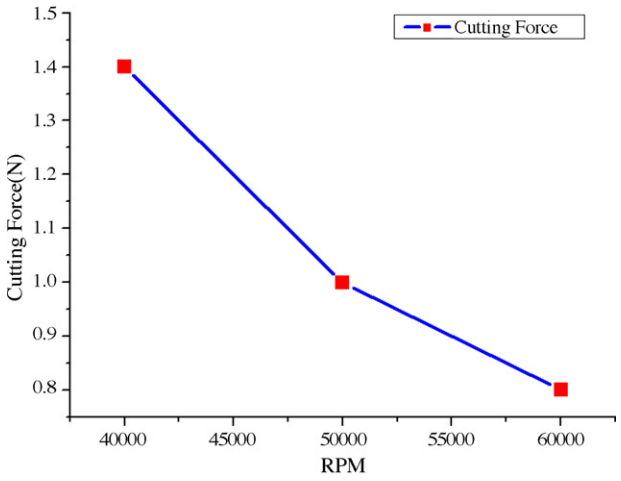

Fig. 12. Cutting force variations according to spindle rpm.

4. Conclusions

In this study, *R*-curve behavior was analyzed for the machinability evaluation of the Si_3N_4-hBN composites. Higher hBN content in the composites resulted in more slowly rising *R*-curves, which could enhance machinability. Micro-machining processes were performed to evaluate the machinability, and the results can be summarized as follows:

(1) In the micro-shaping process of the Si_3N_4-hBN composites, higher contents of h-BN and smaller depth of cut can resulted in better V-grooves.
(2) In the micro-grooving process, good results could be obtained for smaller depth of cut and feed rate. However, serious tool wear was observed for the composites with less than 5% of h-BN contents. Such tool damage made the machining process harder regardless of pressing methods to make the composites.
(3) In the micro-barrier making process using micro-end-milling process, good results could be obtained for 20% h-BN composites. However, rough detachment of particles was observed at the cutting-in region of the tool due to brittle fracture. Machinability and machined shapes were very poor for lower h-BN contents in the composites.
(4) In the micro-drilling process, thrust forces decreased as spindle rpm increases.
(5) Such results can be applied to determine the optimum h-BN contents and matching micro-machining process conditions for the Si_3N_4-BN composites to make micro-patterns and shapes.

Acknowledgement

This work was supported by Inha University Research Grant.

References

1. Kawamurs, H., *Key Eng. Mater.*, 1994, **89**, 713–718.
2. Raj, R., Fundamental research in structural ceramics for service near 2000. *J. Am. Ceram. Soc.*, 1993, **76**, 2147–2174.
3. Park, J. S. *et al.*, Cutting characteristics of SiC-based ceramic cutting tools. Part I. Microstructure and mechanical properties of SiC-based cutting tools. *J. KSPE*, 2001, **9**, 82–83.
4. Chyung, K. and Grossman, G., Fluorophlogopite mica glass ceramics. In *Proceedings of the 10th International Congress on Glass*, 1974, pp. 33–40.
5. Beall, G. H., Structure, properties and applications of glass ceramics, advances in nucleation and crystallization in glasses. *Am. Ceram. Soc.*, 1972, 251–261.
6. Chantikul, P., Bennison, S. J. and Lawn, B. R., Role of grain size in the strength and *R*-curve properties of alumina. *J. Am. Ceram. Soc.*, 1990, **73**, 2419–2427.
7. Krause Jr, R. F., Rising fracture toughness from the bending strength of indented alumina beams. *J. Am. Ceram. Soc.*, 1988, **71**, 338–342.
8. Davies, M. A., Evans, C. J., Patterson, S. R., Vohra, R. and Bergner, B. C., Application of precision diamond machining to the manufacture of micro-photonics components. In *Proceedings of SPIE, Lithographic and Micromachining Techniques for Optical Component, Fabrication, Vol 5183*, 2003, pp. 94–108.
9. Taniguchi, N., *Nanotechnology-integrated processing system for ultra-precision and ultra-fine products*. Oxford University Press, 1996.
10. Yuan, Z. J., Zhoo, M. and Dong, S., Effect on diamond tool sharpness on minimum cutting thickness and cutting surface integrity in ultraprecision machining. *J. Mater. Process. Technol.*, 1996, **62**, 327–330.
11. Lee, J. S., Lee, S. L., Lee, D. W., Jung, Y. H. and Chung, W. S., A study on micro-grooving characteristics of planar light-wave circuit and glass using ultrasonic vibration cutting. *J. Mater. Process. Technol.*, 2002, **130–131**, 396–400.